Initial and Post-Initial Code Acquisition in the Non-Coherent Multiple Input/Multiple Output Aided DS-CDMA Downlink

SeungHwan Won, *Student Mamber, IEEE* and Lajos Hanzo, *Fellow, IEEE*

***Abstract*— In this paper we investigate the issues of both initial and post-initial acquisition schemes in the Multiple Input/Multiple Output (MIMO) aided Direct Sequence-Code Division Multiple Access (DS-CDMA) downlink, when communicating over spatially uncorrelated Rayleigh channels. The associated Mean Acquisition Time (MAT) performance trends are characterised as a function of the number of MIMO elements. Furthermore, we characterise both the initial and post-initial acquisition performance as a function of the relevant system parameters. Our findings suggest that increasing the number of transmit antennas in a MIMO aided CDMA system results in combining the low-energy, noise-contaminated signals of the transmit antennas, which ultimately increases the MAT by an order of magnitude, when the Signal-to-Interference plus Noise Ratio (SINR) is relatively low, regardless whether single-path or multi-path scenarios are considered. This phenomenon has a detrimental effect on the performance of Rake receiver based synchronisation schemes, when the perfectly synchronised system is capable of attaining its target bit error rate performance at reduced SINR values, as a benefit of employing multiple transmit antennas. Based upon our analysis justified by information theoretic considerations, our acquisition design guidelines are applicable to diverse NC MIMO assisted scenarios.**

***Index Terms*— initial acquisition, post-initial acquisition, serial search, non-coherent MIMO system.**

I. INTRODUCTION

A variety of schemes employing multiple antennas in the DownLink (DL) of wireless systems constitute an attractive technique of reducing the detrimental effects of time-variant multi-path fading environments [1]. In inter-cell synchronous CDMA systems the Mobile Station's (MS) receiver must be capable of perfectly synchronously aligning a locally generated PseudoNoise (PN) code with the received multi-user signals containing the desired user's PN sequence [2], [3]. Our investigations consider the initial synchronisation stage of CDMA systems, aiming for the acquisition of the coarse timing of the signals received in the DL. Therefore our objective is to minimise the Mean Acquisition Time (MAT), which is proportional to both the correct detection probability (P_D) as well as to the time required by the acquisition scheme to notice after the elapse of the code phase verification period that a false locking event occured and hence to return to the search mode. The uncertainty region in the DL corresponds to the entire period of the PN sequence, which tends to be quite wide, for instance $(2^{15}-1)$ chip intervals in the DL of the inter-cell synchronous CDMA system [2],[4]. Therefore the MAT is minimised in the context of serial search techniques by achieving the best possible P_D, whilst maintaining as low a value of the false alarm probability (P_F) and false locking penalty as possible. However, most of these acquisition schemes have been designed for single transmit/single receive antenna aided systems, with the aim of optimising the achievable MAT performance. Furthermore, there is a paucity of code acquisition techniques designed for optimum post-initial acquisition performance [5],[6], where the term 'post-initial acquisition [5]' refers to identifying the timing instants of the affordable-complexity-dependent number of delayed received signal paths, which will be combined by Rake receiver.

The substantial appeal of MIMOs is that their capacity increases linearly with the SINR, as opposed to the more modest logarithmic increase of the classic Shannon-Hartley law, which may be simply exemplified by assigning the increased transmit power to an additional antenna and hence linearly increasing the throughput [7]. Ironically, when considering a fixed total power, but increasing the number of transmitter elements, the 'per-element power' is reduced, which potentially results in a degraded acquisition performance, even if the associated degradation is partially compensated by increasing the number of receiver elements. This initial acquisition challenge has not been detailed in journal papers, even though there are thousands of papers on showing the performance improvements of diverse MIMOs in perfect initial synchronisation scenarios. Against this background, in this treatise we investigate serial search based Non-Coherent (NC) code acquisition schemes designed for MIMO aided systems for the sake of analysing the characterisitics of both initial and post-initial acquisition schemes. More explicitly, we quantify both the P_D as well as the P_F as a function of both the SINR per chip and that of the number of MIMO elements. Furthermore, we characterise the attainable MAT versus E_c/I_0 performance parameterised by the number of MIMO elements. Finally, based on our results justified by information theoretic considerations, we provide acquisition design guidelines applicable to diverse NC MIMO aided scenarios.

This paper is organised as follows. Section II describes the system investigated, followed by the P_D and P_F analysis of NC code acquisition schemes in the context of spatially uncorrelated Rayleigh channels, while the MAT analysis of both initial and post-initial acquisition is illustrated in Section III. In Section IV, our numerical MAT results are discussed, while our conclusions are offered in Section V.

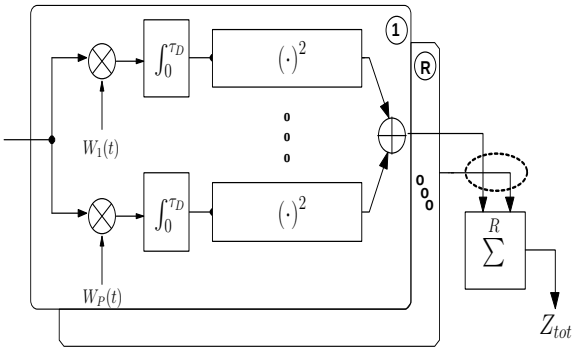

Fig. 1. Receiver structure of a non-coherent code acquisition system employing R receive antennas. Its basic operation is identical for both the initial and post-initial acquisition schemes, except for using different coherent summation intervals necessitated by the different frequency mismatch of the two schemes

II. CORRECT DETECTION AND FALSE ALARM PROBABILITY

We assume that a finite-length tapped delay line channel model generates L Rayleigh-faded multi-path signals, each arriving with a time delay τ_l having a tap spacing of one chip-duration [3],[8], where $l = L$ is the number of multi-path components. It is also assumed that the Rayleigh fading is sufficiently slow for the faded envelope to remain constant over duration of $\tau_D = N{\cdot}T_c$, but fast enough so that the consecutive τ_D-duration segments may be considered essentially independently faded, as in [2],[9],[10], where τ_D indicates the integral dwell time, N represents the number of chips accumulated over the duration of τ_D and T_c is the chip duration. Furthermore, the Neyman-Pearson criterion [2],[11] is adopted, which leads to a constant false-alarm rate. This is because as a benefit of normalising the received signal by the background noise variance estimate, the fading channel's attenuation no longer affects the outcome of a test, whether the desired signal is present or absent. The resultant scenario and the related test becomes reminiscent of an Additive White Gaussian Noise (AWGN) scenario. Consequently, in line with the findings of [2],[9],[10], the mobile channel only affects the P_D peformance. The spacing of both the multiple transmit elements at the BS and the multiple receive elements at the MS are assumed to be 10 λ and 0.5 λ, respectively [12]. Accordingly, it is assumed that there is no spatial correlation among the DL signals emanating from the P transmit antennas. Finally, we note that the analysis of our code acquisition schemes is valid for both spatial division multiplexing [13] and for space-time coding [14] MIMOs.

The signal received over the multi-path Rayleigh fading channel at each receive antenna of the MIMO aided DS-CDMA DL may be expressed as [15]

$$r_n(t) = \sum_{l=1}^{L}\sum_{m=1}^{P}[\alpha_{(l,m,n)}\sqrt{\frac{E_c}{PT_c}}\,c(t+dT_c+\tau_l) \quad (1)$$
$$\cdot W_m(t+dT_c+\tau_l)\exp(2\pi ft+\phi_{(l,m,n)}) + I_{(l,m,n)}(t)],$$

where $m = P$ is the number of transmit antennas, $n = R$ is the number of receive antennas, $\alpha_{(l,m,n)}$ represents the complex-valued envelope of the $(l,m,n)^{th}$ signal path obeying the Rayleigh distribution, E_c denotes the pilot signal energy per PN code chip, $c(t)$ represents a common PN sequence having a cell-specific code-phase offset, d is the code phase offset with respect to the phase of the local code, $W_m(t)$ identifies the specific Walsh code assigned to the m^{th} transmit antenna, f is the carrier frequency and finally, ϕ is the carrier phase of a specific user's modulator. Furthermore, $I_{(l,m,n)}(t)$ is the complex-valued AWGN having a double-sided power spectral density of I_0 at the $(l,m,n)^{th}$ path. Here the total allocated power is equally shared by the P transmit antennas. Fig.1 depicts the block diagram of the NC receiver designed for our code acquisition scheme using MIMO elements, which generates a decision variable by accumulating $(P \cdot R)$ number of independently faded signals observed over a time interval for the sake of improving the P_D in the mobile channel imposing both fading and poor SINR conditions. In Fig.1, the numbers 1 to R surrounded by a circle situated in the upper right-hand corner of the largest box represent a specific receiver branch for each receive antenna. In order to simplify the receiver's structure, we omitted the front-end down converter, the chip-matched filter, as well as the sampler and descrambler of the PN code. Further details on the related schemes may be found in [15].

In order to derive the Probability Density Function (PDF) of the decision variable, let us now consider the effects of both the timing errors τ and those of the total frequency mismatch Δf_t on the received signal. The timing errors are imposed by both the delay of the DL signal received from a mobile channel and the sampling inaccuracy caused by having a finite search step size of $\Delta = T_c/2$. The total frequency mismatch is the sum of the clock-drift-induced frequency mismatch Δf_m between the Base Station's (BS) transmitter and the MS's receiver, as well as of the effect of the Doppler shift, Δf_d. If we take into account a strictly band-limited transmit filter [2], the AutoCorrelation Function (ACF) of the timing error, $R(\tau)$ is expressed as [1]

$$R(\tau) = \frac{\sin(\pi\tau/T_c)}{(\pi\tau/T_c)} \equiv sinc(\tau/T_c), \quad (2)$$

where τ is the arbitrary timing error. Due to the squaring operation in the NC receiver of Fig.1 the square of $R(\tau)$ is considered to be the ACF of the timing errors. Similarly, the DL signal energy reduction expressed as a function of the frequency mismatch after the same squaring operation $(\cdot)^2$ of

[1]The timing error effects imposed are highly dependent on the type of the linear waveform-shaping filter transfer function used, rather than on the type of the spreading codes considered, since without shaping they all exhibit rectangular chips. In our scenario we opted for a strictly bandlimited Frequency-Domain (FD) chip-shaping filter transfer function expressed as $H(f) = \frac{1}{\sqrt{W}}\left[u(f+\frac{W}{2}) - u(f-\frac{W}{2})\right]$, where $u(\cdot)$ denotes the unit step function, f is the frequency in $H(f)$ and W represents the total DS-spread bandwidth [2]. The resultant impulse response, $h(t)$ is given by $h(t) = \int_{-W/2}^{W/2} H(f)exp(2\pi ift)df = \sqrt{W}sin(\pi Wt)/(\pi Wt)$, where $W \equiv 1/T_c$. Therefore without loss of generality, when using the squaring operation seen in Fig.1, we have $X_n = +1$, where $n = 1, 2, ..., N$ and X_n represents a squared chip value at the n^{th} chip position, which effectively eliminates the influence of the polarity on the chip-waveform. When we define the ACF $R(\tau)$ as $\int_{-\infty}^{\infty}|H(f)|^2\cos 2\pi f\tau df$, based upon our assumption of the FD chip-shaping filter, we have Eq.2.

Fig.1 becomes [2]:

$$D(\Delta f_t) \approx sinc^2(N\Delta f_t T_c). \quad (3)$$

Hence, the square of the mean values accumulated over τ_D is given by

$$(\overline{N})^2 = N^2(\frac{E_c}{P})sinc^2(\frac{\tau}{T_c})sinc^2(N\Delta f_t T_c). \quad (4)$$

As a result of the above formulation, the effects of both timing errors and frequency mismatches are encapsulated by the definition of the squared mean, $(\overline{N})^2$ formulated in Eq.4. More explicitly, this means that the effects of both of these detrimental factors are directly involved in the energy value measured at the output of the $(\cdot)^2$ block of Fig.1. Accordingly, $(E_c/I_0)'$ is defined as $(E_c/I_0)\cdot sinc^2(\frac{\tau}{T_c})\cdot sinc^2(N\Delta f_t T_c)$, and this definition will be used in the definition of the non-centrality parameter. By employing the procedures proposed in [15] in the context of the receiver structure of Fig.1, the final decision variable of the l^{th} path may be written as

$$\begin{aligned} Z_{tot} &= \sum_{m=1}^{P}\sum_{n=1}^{R} Z_{k(l,m,n)} \quad (5)\\ &= \sum_{m=1}^{P}\sum_{n=1}^{R} \left\| \frac{1}{\sqrt{2}} \left(\sqrt{\frac{4E_c}{NI_0P}} S_{k(l,m,n)} + I_{k(l,m,n)} \right) \right\|^2, \end{aligned}$$

where k denotes the k^{th} chip's sampling instant, $Z_{k(l,m,n)}$ is a decision variable of the $(m,n)^{th}$ path, which constitutes an element of the final decision variable Z_{tot}, $S_{k(l,m,n)} = \frac{1}{T_c}\int_0^{NT_c} c(t)c(t+dT_c+kT_c)\cdot exp(j2\pi N\Delta f_t)dt$. If the PN codes have ideal ACFs, where the ACF has identical sidelobes to those of maximum length shift register sequences [2], $S_{k(l,m,n)}$ can be expressed as $N\cdot exp(j2\pi N\Delta f_t)$ for the signal being present. On the other hand, in case of the signal being absent, it can be shown to be $-1\cdot exp(j2\pi N\Delta f_t)$. Therefore, $S_{k(l,m,n)}$ becomes deterministic [15], while $I_{k(l,m,n)}$ is the complex-valued AWGN having zero means and variances of σ^2=2 for both their real and imaginary parts. Furthermore, $\|\cdot\|^2$ represents the Eucledian norm of the complex-valued argument in Eq.5 and the factor of $1/\sqrt{2}$ is employed in order to normalise according to the noise variance. It is worth noting that the outputs of the squaring operation invoked for both the in-phase and the quadrature branch of $Z_{k(l,m,n)}$ in Fig.1 are modelled as the square of the Gaussian random variable, respectively. Accordingly, the decision variable $Z_{k(l,m,n)}$ of each path obeys a non-central chi-square PDF with two degrees of freedom [3] and having a non-centrality parameter of λ_x, which is either $\frac{2N}{P}(\frac{E_c}{I_0})$ for the hypothesis of the desired signal being present $(H_x, x=1)$ or $\frac{2}{NP}(\frac{E_c}{I_0})$ for it being absent $(H_x, x=0)$ [15]. This PDF is given by [8]

$$f_{Z_{k(l,m,n)}}(z|H_x) = \frac{1}{2}\cdot exp\left[-\frac{(z+\lambda_x)}{2}\right]\cdot \mathcal{I}_0\left(\sqrt{z\cdot\lambda_x}\right), \quad (6)$$

where $z \geq 0$, $x = 0$ or 1 and $\mathcal{I}_0(\cdot)$ is the $zero^{th}$-order modified Bessel function. Our aim is now that of expressing the PDF of a desired user's signal at the output of the acquisition scheme conditioned on the presence of the desired signal in $f_{Z_{tot}}(z|H_x)$ derived for transmission over a spatially uncorrelated Rayleigh channel. In this scenario E_c is multiplied by the square of the Rayleigh-distributed fading amplitude, β, which exhibits a chi-square distribution having two degrees of freedom and it is hence expressed as $f(\beta) = \frac{e^{-\beta/\sigma^2}}{\sigma^2}$, where σ^2 is the variance of the constituent Gaussian distribution. Then the average pilot signal energy $\overline{E_c}$ per PN code chip can be expressed as $\overline{E_c} = \overline{\beta}E_c = \sigma^2 E_c$ [2]. Therefore first the PDF $f_{Z_{k(l,m,n)}}(z|H_x,\beta)$ corresponding to β conditioned on the hypothesis of the desired signal being transmitted over an AWGN channel having this specific SINR is weighted by the probability of occurrence $f(\beta)$ of encountering β, as quantified by the PDF. The resultant product is then averaged over its legitimate range of $-\infty \sim \infty$, yielding:

$$\begin{aligned} f_{Z_{k(l,m,n)}}(z|H_x) &= \int_{-\infty}^{\infty} f(\beta)\cdot f_{Z_{k(l,m,n)}}(z|H_x,\beta)d\beta \quad (7)\\ &= \int_0^{\infty}\left(\frac{e^{-\beta/\sigma^2}}{\sigma^2}\right)\cdot\frac{\exp[-(z+\beta\lambda_x)/2]}{2} \quad (8)\\ &\quad \cdot\mathcal{I}_0\left(\sqrt{\beta\lambda_x z}\right)d\beta\\ &= \frac{\exp[-z/(2+\lambda_x\sigma^2)]}{(2+\lambda_x\sigma^2)} \quad (9)\\ &\equiv \frac{\exp[-z/(2+\overline{\lambda_x})]}{\left(2+\overline{\lambda_x}\right)}, \quad (10) \end{aligned}$$

where the effects of both timing errors and frequency mismatches are encapsulated by the definition of $(\overline{E_c/I_0})'$ and the corresponding noncentrality parameter, $\overline{\lambda_x} \equiv \lambda_x\sigma^2$ is either $\frac{2N}{P}(\frac{\overline{E_c}}{I_0})'$ when the desired signal is deemed to be present $(H_x, x=1)$ or $\frac{2}{NP}(\frac{\overline{E_c}}{I_0})'$ when it is deemed to be absent $(H_x, x=0)$. We also define $\mu_x = (2+\overline{\lambda_x})$, which physically represents a new biased noncentrality parameter. Further details on the related calculations can be found in [2],[15]. Finally, we arrive at the PDF of $Z_{k(l,m,n)}$ conditioned on the presence of the desired signal in the form of:

$$f_{Z_{k(l,m,n)}}(z|H_x) = \frac{1}{\mu_x}e^{-z/\mu_x}. \quad (11)$$

Since the decision variables Z_{tot} is constituted by the sum of $(P\cdot R)$ number of independent variables, which has a PDF given by Eq.11, we can determine the Laplace transform of each by raising them to the $(P\cdot R)^{th}$ power and then carrying out the inverse transform for the sake of generating the desired PDF [2], leading to:

$$f_{Z_{tot}}(z|H_x) = \frac{z^{(PR-1)}e^{-z/\mu_x}}{\Gamma(PR)\cdot{\mu_x}^{PR}}, \quad (12)$$

where $\Gamma(\cdot)$ is the Gamma function. Finally, the probability of correct detection or false alarm corresponding to $\xi = D$ or F, respectively, is obtained as

$$\begin{aligned} P|_{\xi=D\ or\ F} &= \int_{\theta}^{\infty} f_{Z_{tot}}(z|H_x)dz|_{x=1\ or\ 0} \quad (13)\\ &= \exp(-\frac{\theta}{\mu_x})\cdot\sum_{k=0}^{PR-1}\frac{(\theta/\mu_x)^k}{k!}, \quad (14) \end{aligned}$$

where θ is a threshold value.

III. MAT ANALYSIS OF INITIAL AND POST-INITIAL ACQUISITION

The classic serial search techniques designed for initial acquisition [2] have been traditionally employed in specific scenarios, where the uncertainty region (or search window width) is quite wide (i.e. $2^{15}-1$) and the length of the PN sequence in our system was assumed to be $(2^{15}-1)\cdot T_c$, as seen for example in the DL of the inter-cell synchronous CDMA-2000 system [2], where the chip-duration is $T_c = 1/1.2288\mu s$. In the case of initial acquisition contrived for DS-CDMA, the main design goal is to acquire perfect timing of the first received signal path impinging at the receiver, since this timing information is used as that of the reference finger of the Rake receiver. By contrast, the post-initial acquisition procedure that extracts the accurate timing positions of the remaining delayed paths and identifies the appropriate paths earmarked for processing by the maximum ratio combining scheme of the Rake receiver, has a major impact on the performance of the Rake receiver [6]. There are two main differences between the initial and post-initial acquisition procedures. First of all, once the first Rake finger is synchronised, the uncertainty region that has to be explored will be shrunk to $\pm U$ hypotheses surrounding the time-instant, where the first received path was found and U represents the reduced uncertainty region to be explored after the initial acquisition [5]. This search window width is defined by both the dispersion of the multipath propagation environment encountered as well as by the appearance and disappearance of propagation paths [16]. Secondly, the post-initial acquisition procedure commences after automatic frequency control operation was activated for the sake of fine tracking, following the successful initial acquisition. Hence, the performance degradation imposed by the associated frequency mismatch is considerably reduced compared to that immediately after the initial acquisition. Accordingly, these two factors are taken into account in our forthcoming analysis.

In [2],[4], explicit MAT formulae were provided for a single-antenna aided serial search based code acquisition system. There is no distinction between a single-antenna aided scheme and a multiple-antenna assisted one in terms of analysing the MAT, except for deriving the P_D and the P_F based upon the MIMO elements. We will commence our discourse by analysing the MAT performance of both initial and post-initial acquisition schemes employing both Single Dwell Serial Search (SDSS) as well as Double Dwell Serial Search (DDSS). We assume that in each chip duration T_c, α number of correct timing hypotheses are tested, which are spaced by T_c/α. Hence the total uncertainty region is increased by a factor of α. Moreover, as mentioned in Section II, when the L multi-path signals arrive with a time delay τ_l having a tap spacing of one chip-duration, then the relative frequency of the signal being present is increased L-fold. The required transfer functions [2],[4], are defined as follows. The entire successful detection function $H_D(z)$ encompasses all the branches of a state diagram [2],[4], which lead to successful detection. Furthermore, $H_0(z)$ indicates the absence of the desired user's signal at the output of the acquisition scheme, while $H_M(z)$ represents the overall miss probability of a search run carried out across the entire uncertainty region. Since all the nodes of the state diagram are assumed to be a priori equally likely, the resultant transfer function averaged over all the $(\nu - 2\alpha L)$ root-nodes or starting-nodes becomes [2],[4]

$$T(z) = \frac{1}{(\nu - 2\alpha L)} \sum_{i=1}^{(\nu-2\alpha L)} \frac{H_0^i(z) H_D(z)}{[1 - H_M(z) H_0^{(\nu-2\alpha L)}(z)]} \quad (15)$$

$$= \frac{H_D(z) H_0(z) [1 - H_0^{(\nu-2\alpha L)}(z)]}{(\nu - 2\alpha L)[1 - H_0(z)][1 - H_M(z) H_0^{(\nu-2\alpha L)}(z)]}. \quad (16)$$

Eq.16 encompasses an average of all the information regarding both the time instant and the probability of the i^{th} path in the resultant transfer function. By employing the differentiation of $T(z)|_{z=1}$, it may be shown that the generalised expression derived for computing the MAT of the serial search based code acquisition scheme is given by [2],[3],[4]:

$$E[T_{ACQ}] = \frac{1}{H_D(1)} [H_D{}'(1) + H_M{}'(1) + \quad (17)$$

$$\{(\nu - 2\alpha L)[1 - \frac{H_D(1)}{2}] + \frac{1}{2} H_D(1)\} H_0{}'(1)] \cdot \tau_{D1}$$

$$\approx \frac{(1 + H_M(1)) \cdot H_0{}'(1)}{2 \cdot (1 - H_M(1))} \cdot (\nu \cdot \tau_{D1}), \quad (18)$$

where $H_x'(z)|_{x=D,\, M\, or\, 0}$ is a derivative of $H_x(z)|_{x=D,\, M\, or\, 0}$, ν represents the total number of states to be searched and τ_{D1} denotes the 1^{st} dwell time. The related processes are further detailed for SDSS in [2] and for DDSS in [4],[17],[18]. The exact MAT formula can be simplified, if ν is significantly higher than the number of H_D states [3]. In order to simplify our numerical performance analysis, we adopted the approximation of the exact MAT expression proposed in [3]. Since each resolvable path contributes two hypotheses of the signal being present and because the average P_D associated with these two hypotheses is the same, the overall miss probabilities of both the SDSS and the DDSS schemes may be expressed as:

$$H_M(1) = \prod_{l=1}^{L} \prod_{\zeta=1}^{\alpha} (1 - P_{D(l,\zeta)})^2 \quad and \quad (19)$$

$$H_M(1) = \prod_{l=1}^{L} \prod_{\zeta=1}^{\alpha} [(1 - P_{D1(l,\zeta)}) + P_{D1(l,\zeta)} \cdot (1 - P_{D2(l,\zeta)})]^2,$$

respectively, where $P_{D(l,\zeta)}$ represents the correct detection probability of the SDSS scheme and $P_{Dx(l,\zeta)}|_{x=1,\, or\, 2}$ are the correct detection probability of both the search and the verification modes of the DDSS arrangements, respectively. Both $P_{D(l,\zeta)}$ and $P_{Dx(l,\zeta)}$ are given by Eq.14, provided that the condition of the signal being present is satisfied. The $H_0{}'(1)$ values of the SDSS and DDSS schemes are expressed as:

$$H_0{}'(1) = ,1 + K \cdot P_F \quad and \quad (20)$$

$$H_0{}'(1) = 1 + m \cdot P_{F1} + K \cdot P_{F1} \cdot P_{F2},$$

respectively, where K denotes the false locking penalty factor expressed in terms of the number of chip intervals required

by an auxiliary device for recognising that the code-tracking loop is still unlocked and m represents the exponent of z in the verification mode. Furthermore, P_F is the false alarm probability of the SDSS scheme and $P_{Fx}|_{x=1,\,or\,2}$ represent the false alarm probability in both the search and in the verification mode of the DDSS scheme, respectively. Similarly, both P_F and P_{F_x} are given by Eq.14, provided that the condition of the signal being absent is satisfied.

IV. NUMERICAL SYSTEM PERFORMANCE RESULTS

TABLE I

MAXIMUM SINR DEGRADATION INFLICTED BY BOTH THE DOPPLER SHIFT AND A 1000HZ FREQUENCY MISMATCH IN CONJUNCTION WITH THE COHERENT INTEGRATION INTERVAL OF N CHIP DURATIONS AT A CARRIER FREQUENCY OF 1.9GHZ

N(Chips)	64	128	256	384	512
Degradation(dB)	0.061	0.2449	0.9969	2.3144	4.3213

TABLE II

MAXIMUM SINR DEGRADATION INFLICTED BY BOTH THE DOPPLER SHIFT AND A 200HZ FREQUENCY MISMATCH IN CONJUNCTION WITH THE COHERENT INTEGRATION INTERVAL OF N CHIP DURATIONS AT A CARRIER FREQUENCY OF 1.9GHZ

N(Chips)	128	256	384	512	640	768
Degradation(dB)	0.032	0.128	0.289	0.5159	0.812	1.179

In this section we will characterise the MAT performance of the MIMO aided DS-CDMA code acquisition scheme of Fig.1. In Tables I and II we outlined the maximum SINR degradation imposed by both the Doppler shift and the frequency mismatch between the transmitter and receiver in conjunction with the coherent integration interval of τ_D durations seen in Fig.1 for both initial and post-initial acquisition. In the case of the initial acquisition scheme of Fig.1, it was found to be sufficient to integrate the detector output seen in Fig.1 over N =128 chips for the sake of analysing SDSS, while the number of chips over which the accumulator Σ of Fig.1 sums the $(\cdot)^2$ envelope detector's output in both the search and the verification modes of DDSS is assumed to be 32 and 256 in the R = 1 receive antenna scenario or 128 in the R = 4 receive antennas scenario, respectively. By contrast, in the case of the post-initial acquisition scheme, the appropriate length of coherent summation of the detector output values invoked for the sake of analysing SDSS is given in Table III, whilst 64 is selected as the length of coherent summation in the search mode of DDSS. Finally, the appropriate intervals of the coherent summation used in the verification mode of DDSS are portrayed in Table IV. In both Tables III and IV, the numbers seen in $(\cdot)$ can be used as an altenative. These beneficially chosen parameter values were calculated by using the results of both Tables I and II based on Eq.3 as well as taking into account the effects of the sampling inaccuracy, quantified on the basis of Eq.14 and Eq.16 and then finding the parameter values, which resulted in the best achievable MAT performance. The spreading factor of the Walsh code to be acquired was selected to be 128. The frequency mismatch was assumed to be 1000Hz for the initial acquisition [2] and 200Hz for the post-initial acquisition phases [6], while the carrier frequency was 1.9GHz. As a worst-case mobile speed, it is reasonable to postulate 160 km/h. We also assumed that the sampling inaccuracy caused by having a finite, rather than infinitesimally low search step size of $\Delta = T_c/2$ was -0.91 dB, which is a typical value for the search step size [2]. Indeed, when considering multiple hypothesis tests per chip, the effects of cell correlations become non-negligible [19]. However, in case of $\Delta = T_c/2$, the effect of cell correlation becomes modest [19], hence it is reasonable to assume that two consecutive cells are uncorrelated. The total uncertainty regions of the initial and post-initial acquisition were assumed to entail 65534 and 124 hypotheses, respectively. In the spirit of [4], the false locking penalty factor was assumed to be 1000 chip durations. Finally, both single-path and multi-path scenarios were considered. Three paths arriving with a relative time delay of one chip and having a magnitude difference of 3dB, respectively, were assumed to be present in a given search window. All the performance curves have been obtained at the decision threshold of $E_c/I_0 = -13dB$ optimised for the initial acquisition scheme and at $E_c/I_0 = -19dB$ invoked for the post-initial acquisition scheme, respectively. The operational range of the post-initial acquisition scheme was assumed to be 6 dB lower than that of the initial acquisition arrangement, because the signal power of the delayed paths is typically lower than that of the first received path.

TABLE III

OPTIMISED LENGTH OF COHERENT SUMMATION OF DETECTOR OUTPUTS INVOKED FOR THE SAKE OF ANALYSING SDSS IN POST-INITIAL ACQUISITION

Tx/Rx	P1R1	P2R1	P4R1	Tx/Rx	P1R4	P2R4	P4R4
Length (Chips)	512	512	640	Length (Chips)	256 (128)	256 (384)	384

TABLE IV

OPTIMISED LENGTH OF COHERENT SUMMATION OF DETECTOR OUTPUTS INVOKED IN THE VERIFICATION MODE FOR THE SAKE OF ANALYSING DDSS IN POST-INITIAL ACQUISITION

Tx/Rx	P1R1	P2R1	P4R1	Tx/Rx	P1R4	P2R4	P4R4
Length (Chips)	384	640	768	Length (Chips)	256 (384)	384	512

Fig.2 illustrates the achievable MAT versus SINR per chip performance for SDSS of the initial acquisition scheme as a function of the number of transmit antennas for P = 1, 2 as well as 4 and that of the number of receive antennas for R = 1 and 4. In the results of Fig.2 to Fig.6 except for Fig.4, the bold lines indicate the scenario of encountering three paths (denoted as $L3$ in Figs.2 to 6, except for Fig.4), whereas the thinner lines represent a single-path scenario (denoted as $L1$ in Figs.2 to 6, except for Fig.4). Observe in Fig.2 that somewhat surprisingly, as the number of transmit antennas is decreased, despite the potentially reduced transmit diversity

gain, we experience an improved MAT performance for both the single-path and multi-path scenarios. Since the number of states when the signal is present was increased by a factor of L = 3, the MAT performance of this scenario becomes better than that of the single-path one. In the case of R = 4 receivers the performance improvements due to having multiple paths become marginal, because the receive diversity gain is already sufficiently high for having a near-Gaussian MAT-performance. Hence the results of the multi-path scenario of R = 4 were omitted in order to avoid obfuscating details. For comparison, Fig.3 characterises the MAT versus SINR per chip performance of DDSS for the initial acquisition arrangement as a function of the number of transmit antennas for P = 1, 2 as well as 4 and that of the number of receive antennas for R = 1 and 4. Similarly to the conclusions of Fig.2, as the number of transmit antennas is decreased, all the curves seen in Fig.3 illustrate an improved MAT peformance, except that a useful transmit diversity gain is experienced only for the case of $'P2R1'$, and even this gain was limited to the specific SINR range of -4 and -11 dB in the single-path scenario. In the case of DDSS, the performance improvements obtained for the three-path scenario are less than those of SDSS. It is worth mentioning that although not explicitly shown in Figs.2,3,5 and 6 for avoiding obfuscating details, the operating range of R = 2 receive antennas was found to be between that corresponding to the R = 1 and R = 4 receive antenna scenario. To illustrate the above fact a little further, in the case of $'P2R1'$ the DDSS scheme exhibits a better MAT peformance in comparison to the $'P1R1'$ arrangement across the specific SINR range shown in Fig.3. This is because in the case of DDSS the reliable operational ranges in terms of both the correct detection and the false alarm probability are quite different from those of SDSS. More explicitly, the reliable operational range of SDSS associated with the best possible MAT performance is around a false alarm probability of 10^{-4}. On the other hand, the reliable operation of DDSS may be maintained at as high a false alarm probability, as 0.2 when the number of transmit antennas is increased from P=1 to P=4 in conjunction with R=1 receive antenna, as demonstrated in Fig.4. Furthermore, in case of R=4 receive antennas, similar trends are observed, even though the region of the reliable DDSS operation is shifted to the left with respect to the case of a single receive antenna, as seen in Fig.4. It is worth mentioning that the operating range of R = 2 receive antennas is in between that corresponding to R = 1 and R = 4 receive antennas, for the sake of avoiding obfuscating points in the figure, the R = 2 scenario was omitted. Accordingly, while the reliable operational range of SDSS is around a false alarm probability of 10^{-4}, that of DDSS in the search mode varies more widely, namely across the range spanning from 0.04 to just over 0.2, depending on the specific number of MIMO elements. This manifests itself also in terms of having detection threshold values in the search mode of DDSS, which are substantially lower than those of SDSS, when optimised for the sake of attaining the best possible MAT performance. This clearly implies that DDSS benefits from a significantly higher diversity gain than SDSS. The peformance degradation imposed by employing multiple antennas becomes more drastic, as the number of transmit antennas is increased for both the SDSS and DDSS schemes in the initial acquisition scenario. Furthermore, the associated MAT performance discrepancy between the SDSS and DDSS schemes becomes more drastic. In case of employing both multiple transmit and multiple receive antennas, similar trends are observable, although using four receive antennas has the potential of mitigating the associated acquisition performance degradation imposed by the low per-branch E_c/I_0 values associated with the employment of multiple transmitters.

Fig.5 and Fig.6 characterise the achievable MAT versus SINR per chip performance of post-initial acquisition. The results are parameterised by both the number of transmit antennas for P=1, 2 as well as 4 and by the number of receive antennas for R = 1 as well as 4 for both the SDSS (Fig.5) and for the DDSS schemes (Fig.6), respectively. Even though the optimised coherent summation intervals determined for the sake of obtaining the best possible MAT performance are quite different, as the number of transmit antennas is decreased, all the curves seen in both Fig.5 and Fig.6 indicate an improved MAT peformance, as we observed in the case of intial acquisition in both Fig.2 and Fig.3. This trend explicitly indicates that the DDSS scheme also degrades the achievable MAT performance as a consequence of the low per-antenna power imposed by employing multiple transmit antennas for the sake of attaining a transmit diversity gain. However, the MAT peformance degradation imposed is less severe than that of the SDSS scheme. Moreover, the performance improvements of the initial acquisition scheme recorded for SDSS in Fig.2 as a benefit of having multiple paths is more significant than those of the post-initial acquisition arrangement shown for SDSS in Fig.5. The initial acquisiton scheme having multiple received paths contributes to the attainable performance improvements. On the other hand, in the case of DDSS, the performance improvements obtained for the three-path scenario are lower than those of SDSS in both the initial and post-initial acquisition scenarios. The performance improvements due to having multiple paths become the lowest for the post-initial acquisition arrangement using DDSS in Fig.6. To interpret all the above results a little further, a low level of per-branch received signal strength would lead to a low acquisition performance, despite achieving a high transmit diversity gain. In other words, a high transmit diversity order effectively results in an acquisition performance loss, as a consequence of the insufficiently high signal strength per transmit antenna branch.

Based on the above-mentioned analysis, the detrimental factors governing the best attainable MAT performance are classified according to 1) the value of the clock-drift-induced frequency mismatch and 2) the number of transmit antennas. By contrast, the beneficial factors are categorised according to the following four classes: 1) the length of coherent summation, 2) the number of receive antennas, 3) the number of multi-path components and 4) the number of dwell intervals. The main reasons for the above-mentioned performance trends may be further justified by a number of information theoretic considerations applied to the NC MIMO aided scenarios as follows [20],[21],[22]:

Wireless systems employing MIMOs exhibit a high capacity, provided that the channel is known to the receiver [23]. By contrast, a NC MIMO aided scheme, which does not rely on any channel knowledge has a lower capacity [20],[21],[22]. However, it was argued in [21] that there is no reason for using more than $T_S/2$ number of transmit antennas, where based on the results of both Tables I and II $T_S = 2$ was the number of symbols over which integration is carried out, because the number of degrees of freedom increases with $T_S/2$, but only until P approaches $T_S/2$ [21], where P is the number of transmit antennas. Furthermore, at low SINRs the mutual information between the transmitter and receiver is maximised by using a single transmit antenna, because the mutual information bounds were shown to be decreasing functions of P [22]. This implies that using multiple transmit antennas provides no MAT performance gain in the low SINR region, it rather leads to an MAT performance degradation. Finally, in the medium SINR range a maximum of T_S transmit antennas is worth employing for the sake of achieving an MAT performance gain, because the capacity achieved for $P > T_S$ is the same as that achieved for $P = T_S$ [20]. This indicates that $P = 2$ transmit antennas are capable of achieving an improved MAT performance in the SINR region of -4 and -11 dB in the single-path scenario of Fig.3. Finally, when considering the design of MIMO aided code acquisition schemes, the following guidelines may be inferred:

a) Using multiple transmit antennas typically leads to an MAT performance degradation, except for the $'P2R1'$ scenario encountering a single-path environment. Using a relatively low number of chips, over which integration or accumulation is carried out imposes further limits on the attainable benefits of MIMOs. Furthermore, in the multi-path scenarios considered all the results fail to show a transmit diversity gain. Therefore, employing a single transmit antenna might be recommended for maximising the achievable performance of both the initial and post-initial acquisition schemes investigated. Furthermore, using a sufficiently high number of Post-Detection Integration (PDI) stages is also beneficial for minimising MAT [2].

b) Using multiple receive antennas increases the achievable receiver diversity gain and has the potential of compensating for the MAT degradation imposed by the low per-branch power of multiple transmitters.

c) For the sake of acquiring the exact timing information of the received paths, specificially designed preambles, such as that of the primary synchronization channel of W-CDMA [24] combined with time-switched transmit diversity might be recommended, which is capable of achieving a diversity gain with the aid of a single transmit antenna [21],[22]. In practical scenarios, the received path timing differences of the signals arriving from multiple transmit antennas might be distributed within a fraction of a chip duration [25], although they may vary owing to the time-variant propagation delay, hence using multiple transmit antennas may degrade the performance further. In addition to initial acquisition, the classic pilot channel may also be used for carrier frequency error correction and channel estimation.

[2]The underlying philosophy of PDI is that a decision variable is generated by accumulating T consecutive N-spaced signal smaples observed over multiple N-spaced time intervals to improve the P_D in the mobile channel imposing both fading and poor SINR conditions. This specific number must be determined by satisfying a pair of targeted P_D and P_F values for the sake of minimising the MAT.

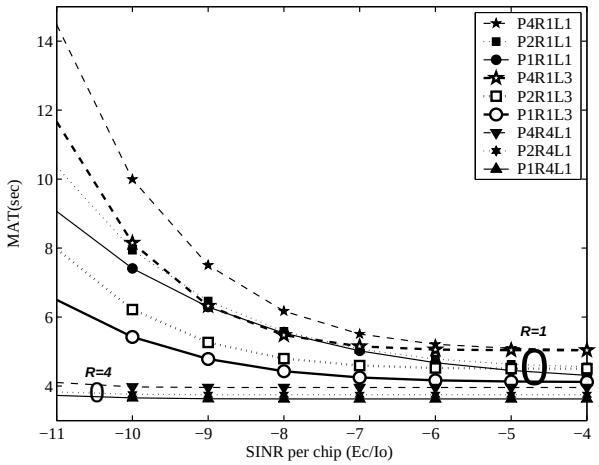

Fig. 2. MAT versus SINR per chip performance of the initial acquisition system for SDSS parameterised with both the number of transmit and receive antennas.

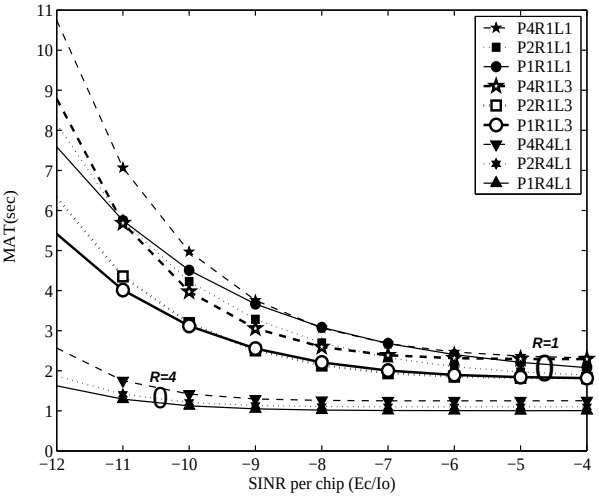

Fig. 3. MAT versus SINR per chip performance of the initial acquisition system for DDSS parameterised with both the number of transmit and receive antennas.

V. CONCLUSION

In this paper, we analysed the MIMO aided diversity effects on the performance of both initial and post-initial acquisition schemes in the inter-cell synchronous CDMA DL. The probabilities of correct detection and false alarm have been derived analytically and numerical results were provided in terms of the attainable MAT performance. Ironically, our findings suggest that increasing the number of transmit antennas in CDMA system results in combining the low-energy, noise-contaminated signals of the transmit antennas, which ultimately degrades the achievable MAT performance, when

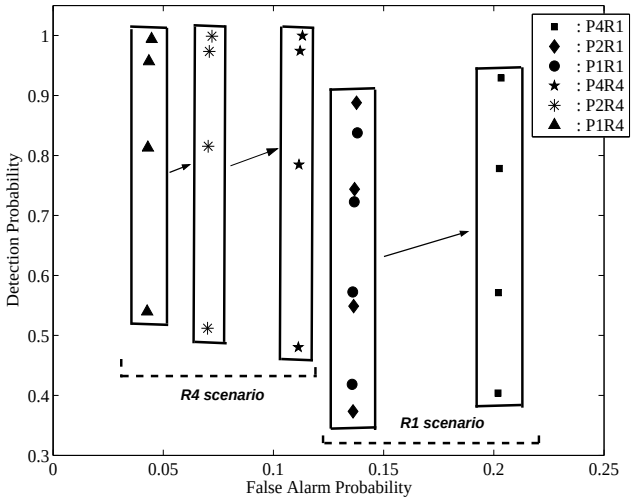

Fig. 4. Operating ranges in the search mode of the initial acquisition scheme for the sake of obtaining the best possible MAT performance. The four vertically stacked points seen in the figure correspond to E_c/I_o = -4, -7, -10 and -13 dB, respectively, from the top to the bottom.

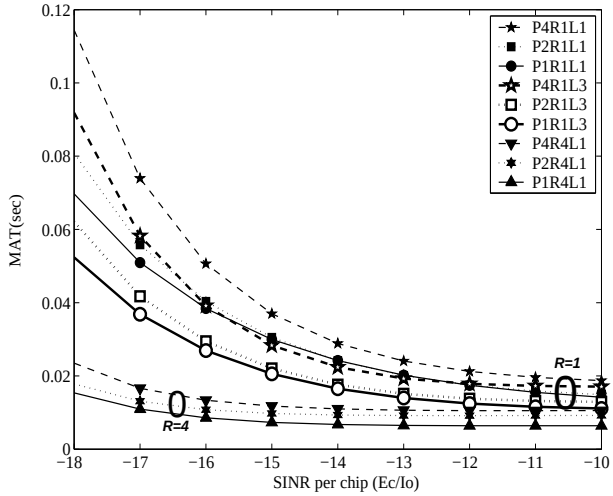

Fig. 6. MAT versus SINR per chip performance of the post-initial acquisition system for DDSS parameterised with both the number of transmit and receive antennas.

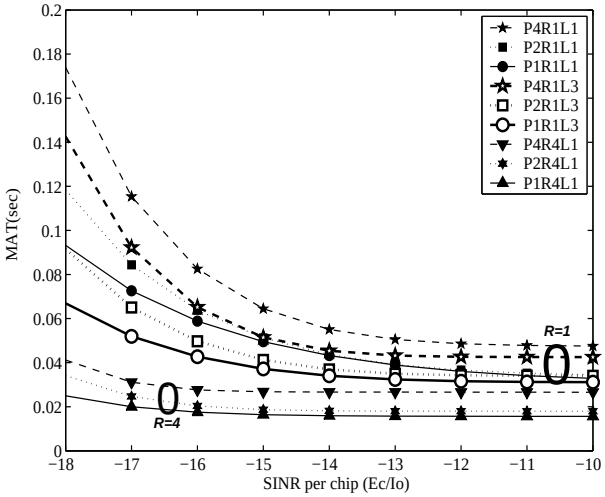

Fig. 5. MAT versus SINR per chip performance of the post-initial acquisition system for SDSS parameterised with both the number of transmit and receive antennas.

the SINR is relatively low, regardless whether single-path or multi-path scenarios are considered. This phenomenon has a detrimental effect on the attainable performance of Rake receiver based initial synchronisation. Based on the above-mentioned results justified by information theoretic considerations, our acquisition design guidelines are applicable to diverse NC MIMO aided scenarios.

ACKNOWLEDGEMENT

The financial support of the Ministry of Information and Communication (MIC), Republic of Korea, of the EPSRC, UK and of the EU is gratefully acknowledged.

REFERENCES

[1] D. Gesbert, M. Shafi, D.S. Shiu, P.J. Smith, and A. Naguib, From Theory to Practice: An Overview of MIMO Space-Time Coded Wireless Systems, IEEE Journal on Selected Areas in Communications, vol. 21, NO.3, Issue 3, 2003, pp281–302.

[2] A.J. Viterbi, CDMA: Principles of Spread Spectrum Communication, Chapter 3, Addison-Wesley, 1995.

[3] L-L Yang, L. Hanzo, Serial Acquisition of DS-CDMA Signals in Multipath Fading Mobile Channels, IEEE Transactions on Vehicular Technology, vol. 50, NO.2, Issue 2, 2001, pp617–628.

[4] H.R. Park, Performance Analysis of a Double-Dwell Serial Search Technique for Cellular CDMA Networks in the Case of Multiple Pilot Signals, IEEE Transactions on Vehicular Technology, vol. 48, NO.6, Issue 6, 1999, pp1819–1830.

[5] S. Glisic, M.D. Katz, Modeling of the Code Acquisition Process for Rake Receivers in CDMA Wireless Networks with Multipath and Transmitter Diversity, IEEE Journal on Selected Areas in Communications, vol. 19, NO.1, Issue 1, 2001, pp21–32.

[6] S.H. Won and Y.J. Kim, Performance Analysis of Multi-path Searcher for Mobile Station in W-CDMA System Employing Transmit Diversity, Electronics Letters, vol. 39, Issue 1, 2003, pp137–139.

[7] S.X. Ng, L. Hanzo, On the MIMO Channel Capacity of Multidimensional Signal Sets, pp528–536, IEEE Transactions on Vehicular Technology, vol. 55, NO. 2, Issue 2, 2006.

[8] J.G. Proakis, Digital Communications, 4th ed. Chapter 2, McGraw-Hill, 2001, pp17–79.

[9] G.E. Corazza, C. Caini, A. Vanelli-Coralli, A. Polydoros, DS-CDMA Code Acquisition in the Presence of Correlated Fading-Part I: Theoretical Aspects, IEEE Transactions on Communications, vol. 52, NO. 7, 2004, pp1160–1168.

[10] G.E. Corazza, C. Caini, A. Vanelli-Coralli, A. Polydoros, DS-CDMA Code Acquisition in the Presence of Correlated Fading-Part II: Application to Cellular Networks, IEEE Transactions on Communications, vol. 52, NO. 8, 2004, pp1397–1407.

[11] R.N. McDonough, A.D. Whalen, Detection of Signals in Noise, 2nd ed. Chapter 5, Academic Press, Inc., 1995.

[12] S. Kim, Effect of Spatial Fading Correlation on CDMA Code-Acquisition Performance, IEE Proceedings - Communication, Vol.152, NO. 1, 2005, pp103–112.

[13] L. Hanzo and M.Münster and B.J. Choi and T.Keller, OFDM and MC-CDMA for Broadcasting Multi-User Communications, WLANs and Broadcasting, John Wiley & Sons, 2003.

[14] V. Tarokh, A. Naguib, N. Seshadri, and A. R. Calderbank, Space-Time Codes for High Data Rate Wireless Communication: Performance Criteria in the Presence of Channel Estimation

Errors, Mobility, and Multile Paths, IEEE Transactions on Communications, vol. 47, NO.2, 1999, pp199–207.
[15] J-C Lin, Differentially Coherent PN Code Acquisition with Full-Period Correlation in Chip-Synchronous DS/SS Receivers, IEEE Transactions on Communications, vol. 50, NO.5, Issue 5, 2002, pp698–702.
[16] 3GPP TS 25.101 V4.11.0, User Equipment (UE) Radio Transmission and Reception (FDD)
[17] H.-C. Wang and W.-H. Sheen, Variable Dwell-Time Code Acquisition for Direct-Sequence Spread-Spectrum Systems on Time-Variant Rayleigh Fading Channels, IEEE Transactions on Communications, vol.48, NO.6, 2000, pp1037–1046.
[18] O.S. Shin and K.B. Lee, Differentially Coherent Combining for Double-Dwell Code Acquisition in DS-CDMA Systems, IEEE Transactions on Communications, vol.51, NO.7, 2003, pp1046–1050.
[19] W.-H. Sheen, J.-K. Tzeng and C.-K. Tzou, Effects of Cell Correlations in A Matched-Filter PN Code Acquisition for Direct-Sequence Spread-Spectrum Systems, IEEE Transactions on Vehicular Technology, vol. 48, NO.3, 1999, pp724–732.
[20] T.L. Marzetta, B.M. Hochwald, Capacity of a Mobile Multiple-Antenna Communication Link in Rayleigh Flat Fading, IEEE Transactions on Information Theory, vol. 45, NO.1, Issue 1, 1999, pp139–157.
[21] L. Zheng, D. N.C. Tse, Communication on the Grassmann Manifold: A Geometric Approach to the Noncoherent Multiple-Antenna Channel, IEEE Transactions on Information Theory, vol. 48, NO. 2, Issue 2, 2002, pp359–383.
[22] C. Rao, B. Hassibi, Analysis of Multiple-Antenna Wireless Links at Low SNR, IEEE Transactions on Information Theory, vol. 50, NO. 9, Issue 9, 2004, pp2123–2130.
[23] G.J. Foschini, Layered Space-Time Architecture for Wireless Communication in a Fading Environment When Using Multi-Element Antennas, AT&T Bell Labs. Tech. J., vol. 1, NO. 2, 1996, pp41–59.
[24] Y.-P.E. Wang, T. Ottosson, Cell search in W-CDMA, IEEE Journal on Selected Areas in Communications, vol. 18, NO.8, Issue 8, 2000, pp1470–1482.
[25] S. Fukumoto, K. Higuchi, M. Sawahashi, F. Adachi, Experiments on Space Time Block Coding Transmit Diversity (STTD) in W-CDMA Forward Link, IEICE Transactions on Fundamentals, vol. E84-A, NO. 12, 2001, pp3045–3057.

SeungHwan Won (M'04) received the B.S. and M.S. degrees in Radio Science and Engineering from Korea University, Seoul, Republic of Korea, in 1999 and 2001, respectively. He was a research engineer in Mobile Communication Technology Research Lab, LG Electronics R&D, from January 2001 to September 2004. He was the recipient of the 2004 state scholarship of the Information and Telecommunication National Scholarship Program, Ministry of Information and Communication (MIC), Republic of Korea. Since October 2004, he has been working towards the Ph.D. degree in the Communications Research Group, School of Electronics and Computer Science at the University of Southampton, UK. His major research interests include initial synchronization in non-coherent MIMO aided single- and multi-carrier CDMA, IDMA and OFDMA as well as in iterative synchronization schemes designed for MIMO aided single- and multi-carrier transmission systems.

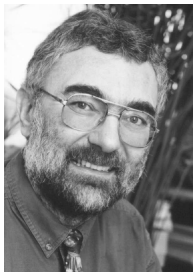

Lajos Hanzo, Fellow of the Royal Academy of Engineering, received his first-class degree in electronics in 1976 and his doctorate in 1983. In 2004 he was awarded the Doctor of Sciences (DSc) degree by the Uniersity of Southampton, UK. During his career in telecommunications he has held various research and academic posts in Hungary, Germany and the UK. Since 1986 he has been with the Department of Electronics and Computer Science, University of Southampton, UK, where he holds the chair in telecommunications. He co-authored 15 John Wiley and IEEE Press books totalling 10 000 pages on mobile radio communications, published about 700 research papers, organised and chaired conference conferences, presented various keynote and overview lectures and has been awarded a number of distinctions. Currently he heads an academic research team, working on a range of research projects in the field of wireless multimedia communications sponsored by industry, the Engineering and Physical Sciences Research Council (EPSRC) UK, the European IST Programme and the Mobile Virtual Centre of Excellence (VCE), UK. He is an enthusiastic supporter of industrial and academic liaison and he offers a range of industrial courses. Lajos is also an IEEE Distinguished Lecturer of both the Communications as well as the Vehicular Technology Society, a Fellow of both the IEEE and the IEE. He is an editorial board member of the Proceedings of the IEEE and a Governer of the IEEE VT Society. For further information on research in progress and associated publications please refer to http://www-mobile.ecs.soton.ac.uk